

# An experimental investigation on the transient heat transfer characteristics using air/water droplets two-phase flow

A H Abed<sup>1,2</sup>, S E Shcheklein<sup>1</sup> and V M Pakhaluev<sup>1</sup>

<sup>1</sup>Ural Federal University named after the first President of Russia B. N. Yeltsin 19 Mira St., Yekaterinburg, 620002, Russia

<sup>2</sup>Department of Electromechanical Engineering, University of Technology, Al-Sina'a St., Baghdad, 10066, Iraq

E-mail: akraaam82@yahoo.com

**Abstract.** The present study focused on evaluating the heat transfer behavior and predicting the surface resulting status during air/water droplets two-phase flow. Transient heat transfer based on the lumped capacitance model (LCM) was investigated experimentally under a range of water droplets concentration, surface temperature, and varying Re number. Compared with a single-phase air cooling, the transient surface temperature decreased with the increase in water droplets concentration and Re number. At the same cooling time, the surface temperature decreases about 13.5%, 47%, and 53.2% for  $(j = 46.79 - 111.68 \text{ kg/m}^2 \text{ hr})$ . It was also noticed that the heat transfer coefficient increased with the increase in water droplets concentration and reach its maximum value at  $(j = 111.68 \text{ kg/m}^2 \text{ hr})$ . Based on the analysis of the experimental results, the heat transfer mechanism due to the impacting of water droplets on the sphere surface was classified into three important physical regimes. Clear convection heat transfer regime corresponds to the dry region (region I); Convection and evaporation regimes correspond to the dry-out and wet regions (region II and III).

## 1. Introduction

Air/water droplets cooling technique applied in numerous industrial and technical processes such as the heat exchanger modules in nuclear and thermal power plants, cooling of electronic and electrical equipment, etc., considered to be an excellent technique and distinguished by the higher heat transfer rate compared with those obtainable by conventional single-phase air cooling [1-5]. These high heat transfer rate occurred due to the phase change of water droplets by the direct evaporation process on the heated surface and absorb a large amount of energy in the form of latent heat, increased the specific heat of mixture, and increased the turbulence inside the thermal boundary layer of the heated surface [6-8]. The air/water droplets heat transfer process is a very complicated phenomenon depends on the several factors such as the water droplet diameter size, the water phase concentration, the flow behavior, the water droplet trajectories, the temperature of the heated surface, and the evaporation time of water droplet on the heated surface. The surface temperature and water phase concentration are important factors that have a great influence on the resulting status of the heating surface (dry, dryout, and wet states) and heat transfer behavior. In the present study, an experimental investigation was performed with an aim to analyze and understand the transient heat transfer behavior of a spherical element cooled using air/water droplets two-phase flow. The estimation of heat transfer behavior during the cooling process was employed based on the lumped capacitance model (LCM).



## 2. The experimental facilities and results treatment

This investigation related to analyzing the heat transfer behavior during the transient -state condition by suspending a fine water droplet on an air main flow. The experimental facilities used in our experiment depicted schematically in figure 1, are the same one was used in references [9, 10]. It consists of the air supply system, water droplets generator system, test specimen, induction heating system, and data acquisition system. The test specimen is represented by a calorimetric copper sphere located inside a cylindrical channel with sphere-to-channel diameter ratio ( $d/D=0.73$ ). The initial working temperature of the test sphere was 100, 200, and 300 °C. The surface temperature was measured by two calibrated (K-type) thermocouples were implanted inside the sphere. The ambient, inlet and outlet fluid temperatures, and the cooling down time were recorded constantly. All thermocouples were connected to the OWEN MV110-8A data acquisition system with MSD200 data logger. A high-frequency heating induction station was used to heat the sphere as a non-contact heating method with output fluctuating frequency 50 - 100 KHz. The average water droplet diameter was ( $dp \leq 10 \mu\text{m}$ ) was obtained by an ultrasonic water droplets generator with 1.7 MHz.

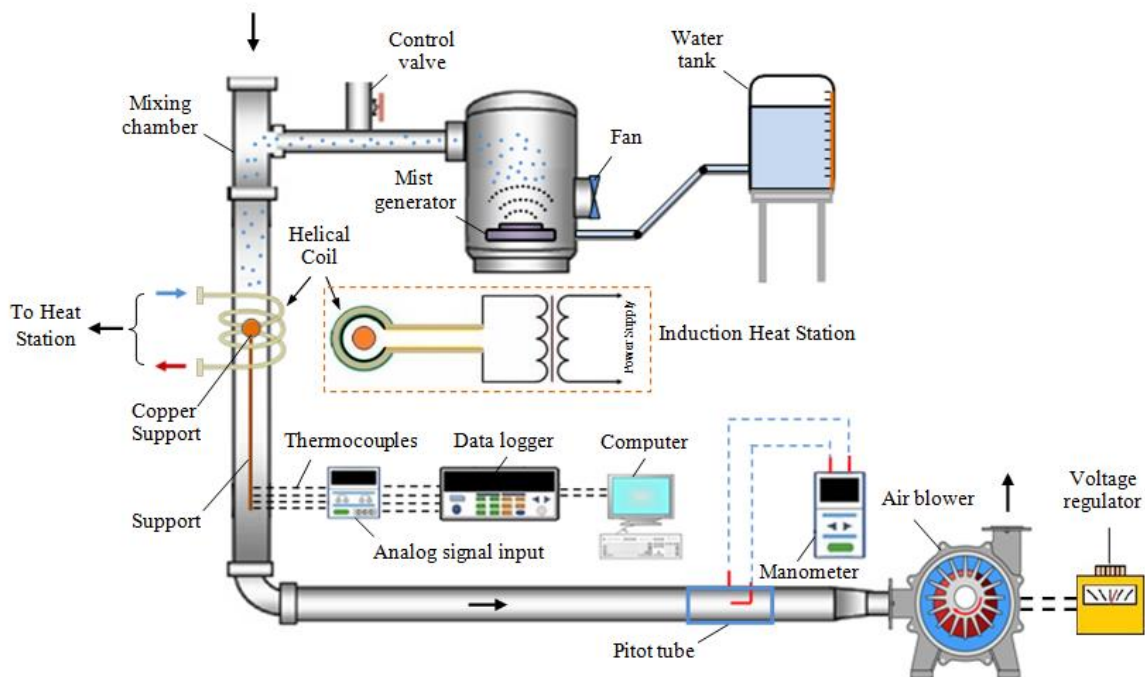


**Figure 1.** Schematic diagram of the experimental facilities.

The experimental tests were performed under a range of water droplets concentration ( $j = 46.79 - 111.68 \text{ kg/m}^2 \text{ hr}$ ) and Re number varying from ( $2.5 \cdot 10^4$  to  $5.5 \cdot 10^4$ ). Firstly, the induction heating system was switched on to heat the test sphere and achieved the required temperature. When the test sphere reached the working temperature, the induction heating system was switched off and the test sphere was exposed to air/water droplets two-phase flows. For Biot number  $\leq 0.1$ , the temperature profile inside the test sphere can be assumed uniform and the lumped capacitance model (LCM) can be employed as a heat transfer evaluate method. Based on the change of internal energy inside the test sphere relating to the convection heat transfer rate at the sphere surface, the general heat conduction equation can be defined as: [11]

$$m_s c_s \frac{\partial T}{\partial t} = h A_s (T_s - T_{in.}) \quad (1)$$

where  $m_s$  and  $c_s$  are the sphere mass, specific heat, and total surface area respectively.  $h$  – is the convection heat transfer coefficient,  $T_{in}$  – is the inlet fluid temperature,  $T_s$  is the temperature inside the sphere,  $t$  – is the cooling time. Eq. (1) was solved analytically and can be written as: [12]

$$h = \frac{C_p \rho d_{sp}}{6} \sum_{i=1}^n \left( \frac{1}{\Delta \tau} \ln \left( \frac{T_{s,i} - T_{in.}}{T_{s,i+1} - T_{in.}} \right) \right) \quad (2)$$

where  $\Delta \tau$  – time difference between two readings of the data logger. The Bi number is defined as: [13]

$$Bi = \frac{hL}{k_s} \quad (3)$$

where  $k_s$  – the thermal conductivity of the sphere and  $L$  – is the characteristic dimension of the sphere, defined as the ratio between the sphere volume  $V_s$  and its total surface area  $A_s$ . The water droplet diameter can be computed by the Lang equation (4), [14-15].

$$d_p = 0.34 \left( \frac{8\pi\sigma}{\rho F^2} \right)^{1/3} \quad (4)$$

### 3. Results and discussion

In order to evaluate the effect of air/water droplets cooling process on the test sphere and predicate the resulting status of the heating surface, there were done the experiments under a range of water droplet concentration ( $j = 46.79 - 111.68 \text{ kg/m}^2 \cdot \text{hr}$ ) and Re number varying from  $(2.5 \cdot 10^4 \text{ to } 5.5 \cdot 10^4)$ . The temperature profile results of the test sphere cooled by air as well as air/water droplets two-phase flow with the initial temperature equal to  $300^\circ\text{C}$  are presented in figure 2.

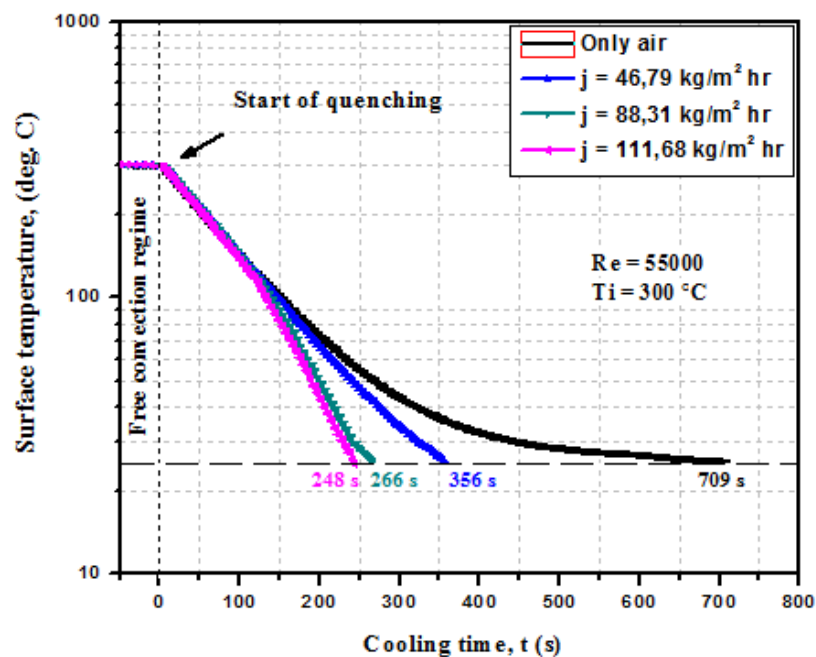


**Figure 2.** Transient cooling curves for different water mist rate at  $Re=55000$ .

Two heat transfer regimes can be distinguished herein. Free convection heat transfer regime occurs when the surface temperature reduced by around 5°C during the water droplet system adjustment to obtain the water droplets concentration required before starting the cooling process. Next, the convective heat transfer was occurred by forced convection. At the starting of quenching, it can be seen that the effect of water droplets on the sphere temperature was insignificant.

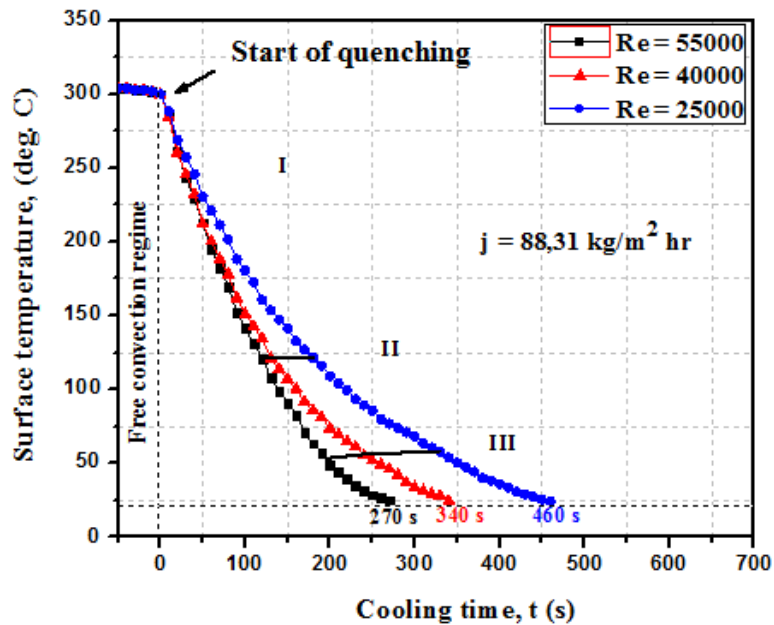


**Figure 3.** Effect of the Re number on the transient surface temperature for range of water droplet concentration ( $j=88.31 \text{ kg/m}^2 \cdot \text{hr}$ ).

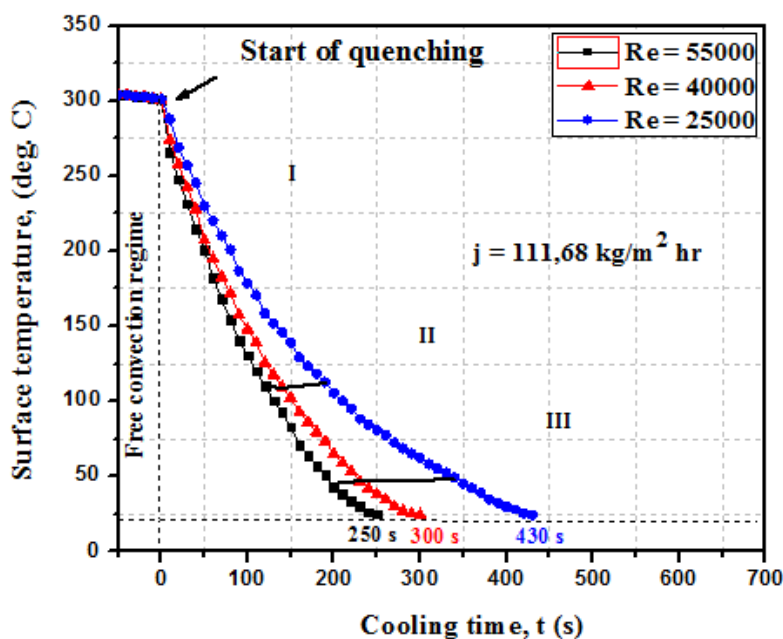


**Figure 4.** Effect of the Re number on the transient surface temperature for range of water droplet concentration ( $j=111.68 \text{ kg/m}^2 \cdot \text{hr}$ ).

It could be associated with the high surface temperature and force of evaporation that leads to evaporate the water droplets before reaching to the sphere surface. After the temperature of sphere reaches to 100°C the influence of water droplets were appear and it can be noticed that the sphere temperature extremely decreases and the cooling time was reduced from 709s for single-phase air cooling to 248s under ( $j = 111.68 \text{ kg/m}^2 \text{ hr}$ ). The surface temperature decreases about 13.5%, 47%, and 53.2% compared with single-phase air cooling under constant Re number. The cooling time for ( $j = 46.79 - 111.68 \text{ kg/m}^2 \text{ hr}$ ) were found to be 50%, 62%, and 65% less than those obtained by ( $j=0 \text{ kg/m}^2 \text{ hr}$ ).

Figures 3 and 4 represents the effect of the air flow velocity in the terms of Reynolds number (Re) on the cooling process by suspending ( $j=88.31 \text{ kg/m}^2 \text{ hr}$ ) water droplets concentration. In our experiments, high Re number which means high flow acceleration that forcing more and more water droplets reaching to the sphere surface and enhance the cooling process by increasing the surface wettability. At the constant cooling time ( $t=250 \text{ s}$ ) the surface temperature decreases about 67% for  $Re=55000$  compared to the surface temperature obtained by  $Re=25000$ . With increasing in water droplets concentration, the number of water droplets impacting on the surface of the sphere also increases that enhances the extraction of heat by absorbing a large amount of energy in form of latent heat during the evaporation process as shown in figures 4. Based on the temperature gradient and direct observation during the glass channel, the cooling curve can be classified according to the resulting states of sphere surface into three different regions as I- dry region, II- dry-out region, and III- wet region as shown in figures (3-6). The effect of the Re number on the transient heat transfer coefficient for a range of water droplet concentration was depicted in figures 5 and 6. For all cases, it can be noticed that the average heat transfer coefficient was drastically increased with increasing of Re number and water droplets concentration. The heat transfer behavior due to the impacting of water droplets on the sphere surface can be classified into three physical regimes. Clear convection heat transfer regime corresponds to the dry region (I - region), convection and evaporation regimes correspond to the dry-out and wet regions (II and III - regions)

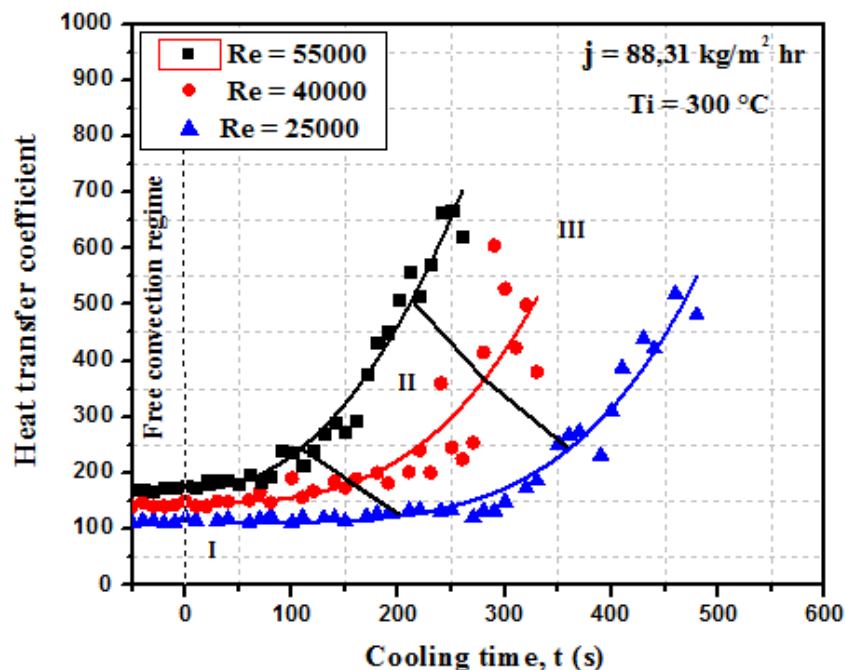


**Figure 5.** Effect of the Re number on the transient heat transfer coefficient for ( $j=88.31 \text{ kg/m}^2 \text{ hr}$ )

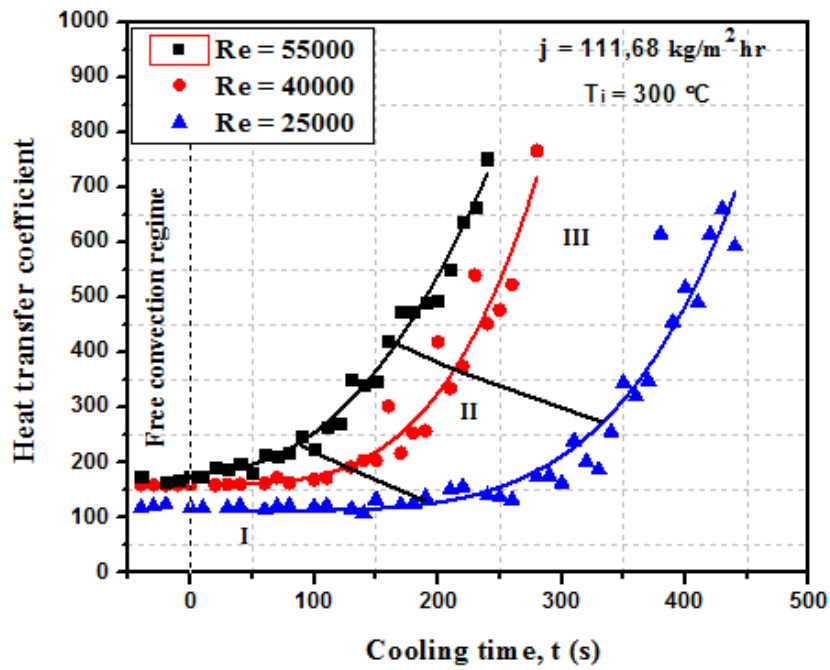


Figure 6. Effect of the Re number on the transient heat transfer coefficient for ( $j=111.68 \text{ kg/m}^2 \text{ hr}$ )

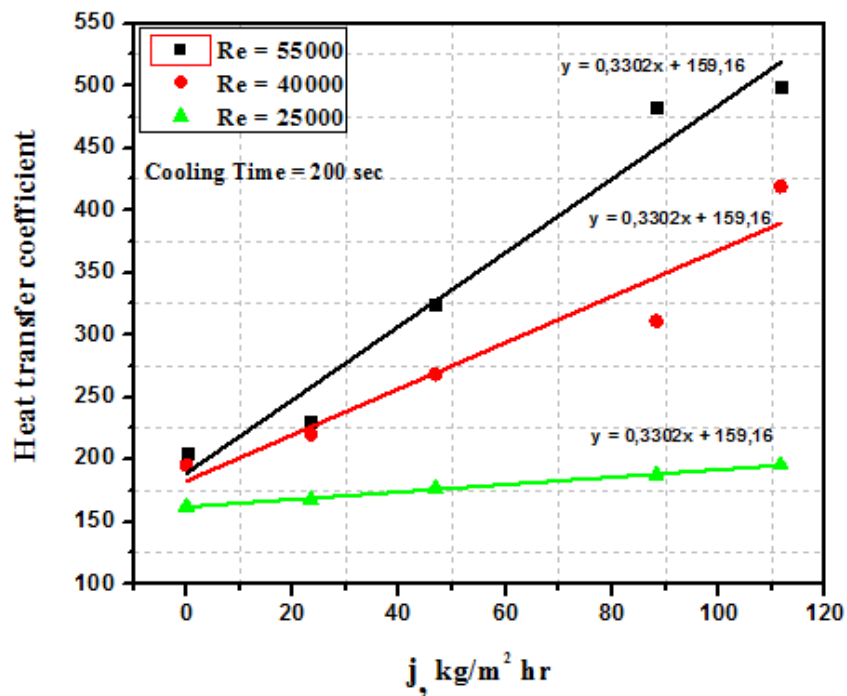
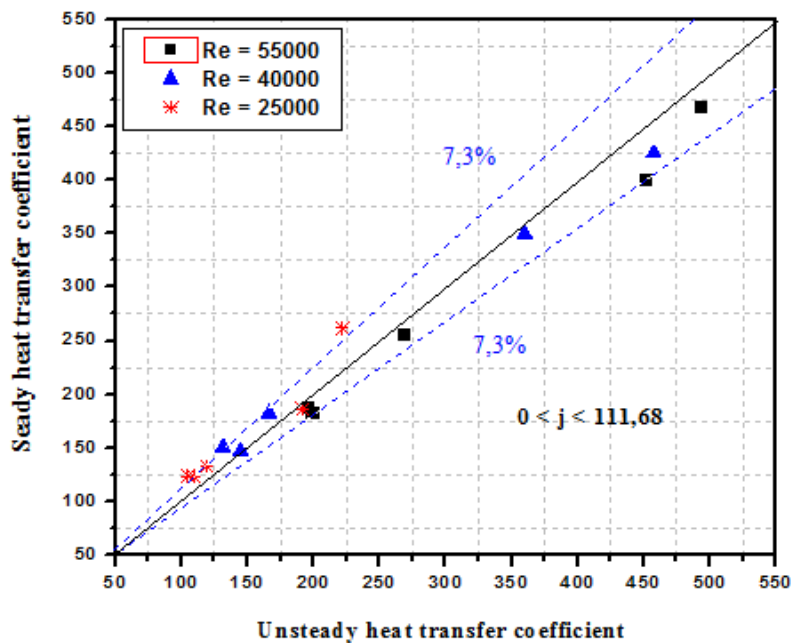


Figure 7. The variations of heat transfer coefficient with water droplets concentration



**Figure 8.** Comparison of steady-state heat transfer coefficient with those obtained by the LCM under corresponding surface temperature conditions.

The variations of heat transfer coefficient with water droplets concentration at constant cooling time (200 sec) is displayed in figure 7. The heat transfer coefficient shows the uptrend with increasing water droplets concentration for all ranges of Re number. In scrutiny of figure 7, the heat transfer coefficient obtained from Re=55000 it's visible to be higher than that obtained by Re=25000 and Re=40000, due to the flow acceleration that forcing more and more water droplets reaching to the sphere surface and enhance the cooling process by increasing the surface wettability as mentioned above. The unsteady-state heat transfer for a varied range of water droplets concentration and different values of Bi numbers were compared with the results obtained by steady-state experiments that were performed in the previous work [9] in terms of corresponding surface temperature of the sphere. The comparison between the steady and unsteady state heat transfer characteristics is shown graphically in figure 8. In this figure, results reasonably agree well within  $\pm 7.3\%$ .

#### 4. Conclusions

In this study, an attempt to analyze and understand the heat transfer behavior during air/water droplets cooling process based on the lumped capacitance model (LCM). The major findings can be reported as follows: suspending water droplets on the air main flow providing a significant reduction on the surface temperature. The surface temperature decreases about 13.5%, 47%, and 53.2% for a range of water droplets concentration ( $j = 46.79 - 111.68 \text{ kg/m}^2 \text{ hr}$ ) compared with single-phase air cooling under constant Re number. The heat transfer mechanism due to the impacting of water droplets on the sphere surface was classified into three important physical regimes. Clear convection heat transfer regime corresponds to the dry region (region I). Convection and evaporation regimes correspond to the dry-out and wet regions (region II and III). Also, the heat transfer coefficient obtained by unsteady and steady heat transfer conditions are compared in terms of the corresponding surface temperature of the sphere with an average deviation of 7.3%.

## References

- [1] Kumari N, Bahadur V, Hodes M, Salamon T, Kolodner P, Lyons A and Garimella S 2010 Analysis of evaporating mist flow for enhanced convective heat transfer *Int. J. Heat Mass Transf.* **53(15-16)** 3346-56
- [2] Agrawal C, Lyons O, Kumar R, Gupta A and Murray D 2013 Rewetting of a hot horizontal surface through mist jet impingement cooling *Int. J. Heat Mass Transf.* **58(1-2)** 188-96
- [3] Sharma A and Sahu S 2019 An experimental study on heat transfer and rewetting behavior of hot horizontal downward facing hot surface by mist jet impingement *Applied Thermal Engineering* **151** 459-74
- [4] Dhanasekaran T and Wang T 2013 Computational analysis of mist/air cooling in a two-pass rectangular rotating channel with 45-deg angled rib turbulators *Int. J. Heat Mass Transf.* **61** 554-64
- [5] Mobtil M, Bougeard D, and Russeil S 2018 Experimental study of inverse identification of unsteady heat transfer coefficient in a fin and tube heat exchanger assembly *Int. J. Heat Mass Transf.* **125** 17-31
- [6] Tan X, Zhang J, Liu B and Zhu X 2013 Experimental investigation on heat transfer enhancement of mist/air impingement jet *Science China Technological Sciences* **56(10)** 2456-64
- [7] Nirmalan N, Weaver J, and Hylton L 1998 An Experimental Study of Turbine Vane Heat Transfer With Water–Air Cooling *J. of Turbomachinery* **120(1)** 50
- [8] Li X, Gaddis J and Wang T 2001 Modeling of Heat Transfer in a Mist/Steam Impinging Jet *J. Heat Transf.* **123(6)** 1086
- [9] Abed A, Shcheklein S and Pakhaluev V 2019 Experimental investigation of hydrodynamics and heat transfer of sphere cooling using air/water mist two phase flow *IOP Conf. Series: Materials Science and Engineering* **552** 012001
- [10] Abed A, Shcheklein S and Pakhaluev V 2019 Investigation of heat transfer coefficient of spherical element using infrared thermography (IR) and gas – water droplets (mist) as working medium *IOP Conf. Series: Materials Science and Eng.* **481** 012033
- [11] Barrow H and Pope C 2007 Droplet evaporation with reference to the effectiveness of water-mist cooling *Applied Energy* **84(4)** 404-12
- [12] Yi D and Zhang M 2017 Heat flux investigations during flame thermal spray process using the lumped capacitance method *Applied Thermal Engineering* **123** 554-61
- [13] Lienhard J H V, Lienhard J H IV 2013 A Heat Transfer Textbook fourth ed. Dover Publications
- [14] Lang R J 1962 Ultrasonic atomization of liquid *Acoust. Soc. Am* **34** 6-8
- [15] Kudo T, Sekiguchi K, Sankoda K, Namiki N and Nii S 2017 Effect of ultrasonic frequency on size distributions of nanosized mist generated by ultrasonic atomization *Ultrasonics Sonochemistry* **37** 16-22